

Article

# Development of Test Equipment for Evaluating Hydraulic Conductivity of Permeable Block Pavements

**Jaehun Ahn** <sup>1</sup>, **Aryssa Kathleen Marcaida** <sup>1</sup>, **Yoongeon Lee** <sup>2</sup> and **Jongwon Jung** <sup>3,\*</sup> <sup>1</sup> Department of Civil and Environmental Engineering, Pusan National University, Busan 46241, Korea; jahn@pusan.ac.kr (J.A.); mkaath@gmail.com (A.K.M.)<sup>2</sup> Eco-Hitec Co., Ltd., Gyeonggi-do 17814, Korea; ecohitek@naver.com<sup>3</sup> School of Civil Engineering, Chungbuk National University, Chungbuk 28644, Korea

\* Correspondence: jjung@chungbuk.ac.kr; Tel.: +82-43-261-2405

Received: 24 May 2018; Accepted: 16 July 2018; Published: 20 July 2018



**Abstract:** The use of permeable block pavement has been acknowledged as one of the promising Low Impact Development (LID) strategies to mitigate the harmful effects of depletion of natural surfaces, due to the uncontrollable development of infrastructure and buildings. Numerous studies, associated with drainage properties and long-term performance of this traditional pavement alternative, have been conducted in the past 30 years. Nevertheless, standardized equipment and methodologies are still limited, specifically for small-scale laboratory models. This paper suggests equipment that is capable of evaluating the hydraulic performance of permeable pavement materials in a laboratory set-up, by monitoring permeability and simulating the physical clogging process. Constant head permeability tests with systematic application of fine clogging particles were conducted on three identical permeable block systems (PBS), composed of four stone pavers. Each test system received an equivalent amount of eight years' particle loading of silica sand, with different size distributions. The experimental results revealed that all the models showed permeability degradation trends similar to those presented in other literature.

**Keywords:** permeable pavement; hydraulic conductivity; constant head test; clogging; permeability equipment; low impact development; permeable block system

## 1. Introduction

The increasing development of infrastructure and buildings have led to the depletion of natural surface coverage, which imposes significant environmental impacts, including serious flooding, increased stormwater pollution, urban heat island effects, and risk to natural ecosystems [1–4]. To alleviate these water-related problems, the demand for stormwater infrastructures and detention facilities have been continuously growing. However, these strategies are considered to be ineffective, primarily due to the limited collection of runoff compared to the larger scale of non-point stormwater sources [4]. Booth and Leavitt [4] have also suggested that detention ponds result in ineffective land use because of the demanding requirements on land area for construction.

To reduce the reliance on traditional stormwater facilities, stormwater management engineers and urban planners have attempted to resolve this issue by managing runoff directly from its source through Low Impact Development (LID) technologies, such as permeable pavement. Permeable pavements have been recognized as a cost-effective source control measure that can reduce discharge peak rates and runoff volumes, which can eventually eradicate the risk of downstream flooding [1,3–6]. This pavement material has also proven its ability to improve water quality by filtering stormwater pollutants, including oils, suspended solids, chemicals, and organic materials [7–11]. As shown in

Table 1, permeable pavements are effective in eliminating suspended solids in particular, having an outstanding 82–95% removal rate [9].

**Table 1.** Pollutant removal by permeable pavement [9].

Study	Pollutant Removal (%)				
	TSS <sup>1</sup>	TP <sup>2</sup>	TN <sup>3</sup>	COD <sup>4</sup>	Metals
Prince William, VA	82	65	80	-	-
Rockville, MD	95	65	85	82	98–99

<sup>1</sup> Total suspended solids, <sup>2</sup> total phosphorus, <sup>3</sup> total nitrogen, <sup>4</sup> chemical oxygen demand.

Among permeable pavement materials, the block pavement system is one of the most common types used as an alternative for conventional pavements (such as concrete and asphalt), and is capable of providing support to traffic loads and draining stormwater. This pavement system consists of an assembly of pre-cast blocks, made of concrete, that are designed with joints, in order to provide drainage through the underlying layers. Stormwater directly infiltrates through the joints, flows through an open-graded bedding substructure, and either drains through the subgrade or through a sewer conveyed by an underdrain [1,2,5,6].

Water permeating through the pavement system generally contains pollutants from vehicular traffic, the surrounding environment, or from the stormwater itself. As these pollutants are being trapped within the joints and layers of the permeable pavement, the drainage performance of the pavement is at risk of failure, until it finally reaches an unacceptable level [6,9,12]. To better understand the clogging and filtration processes within permeable pavements, many studies have been conducted to assess the long-term hydraulic capacity through field and laboratory experiments [6,13–19].

Pezzaniti et al. [6] investigated the effective life of permeable pavement based on laboratory measurements and qualitative field experience (Figure 1). For the laboratory experiments, they simulated the clogging process in three different types of permeable pavements (PPs) by applying locally sourced stormwater. A total of four test beds were studied—two beds containing Boral Formpave (PP1), one bed containing Rocla Ecoloc (PP2), and one bed with Grasspave (PP3).

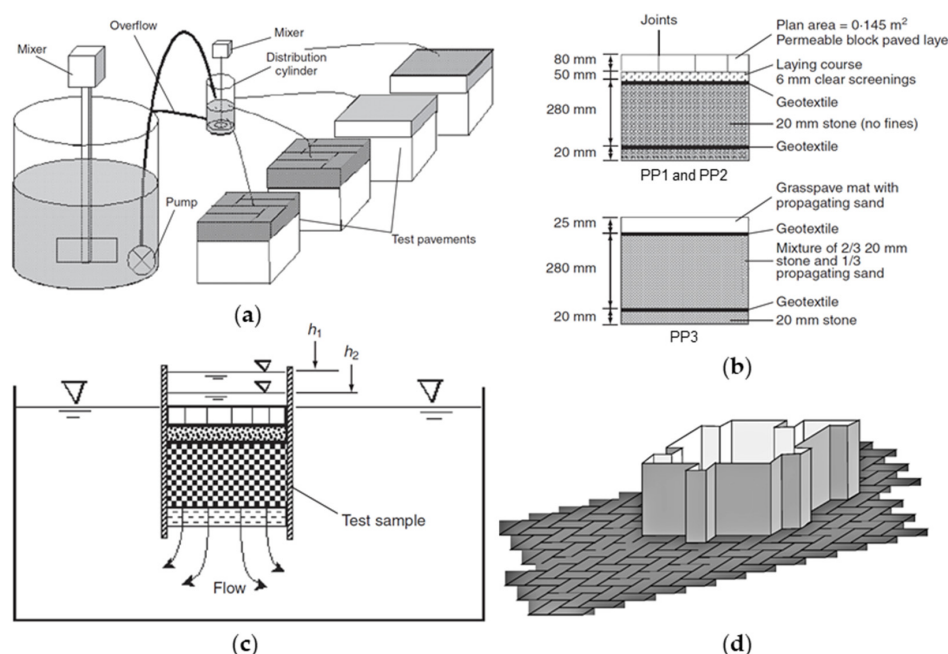


**Figure 1.** Permeable pavement test setup [6]: (a) Test rig for simulating stormwater; (b) test bed cross-section; (c) hydraulic conductivity testing detail; and (d) “fitted tank” apparatus for field testing.

One of the PP1 models was subjected to surface cleaning using a vacuum and brush to simulate real world road-dust sweepers. The other three beds were not cleaned during the experiments. The average annual rainfall in Adelaide is approximately 580 mm, and at a rate of 23.3 L/h, seven hours of constant flow was able to deliver an equivalent of one year's rainfall to the test models. Using an average suspended sediment concentration of 200 mg/L, an estimated equivalent of 35 years of polluted stormwater was delivered using a two-phase mixer. Falling head permeability tests were conducted at five-day intervals to monitor the changes in the hydraulic conductivity of the permeable pavement structures. Laboratory test results showed a rapid decline in the hydraulic conductivity in the first few years of simulation, and a gradual decrease in the latter years. At the end of the sediment loading period, the two PP1 test models exhibited an average hydraulic conductivity reduction of 59%, while the PP2 and PP3 test beds experienced a decline of 68% and 75%, respectively (Figure 2).

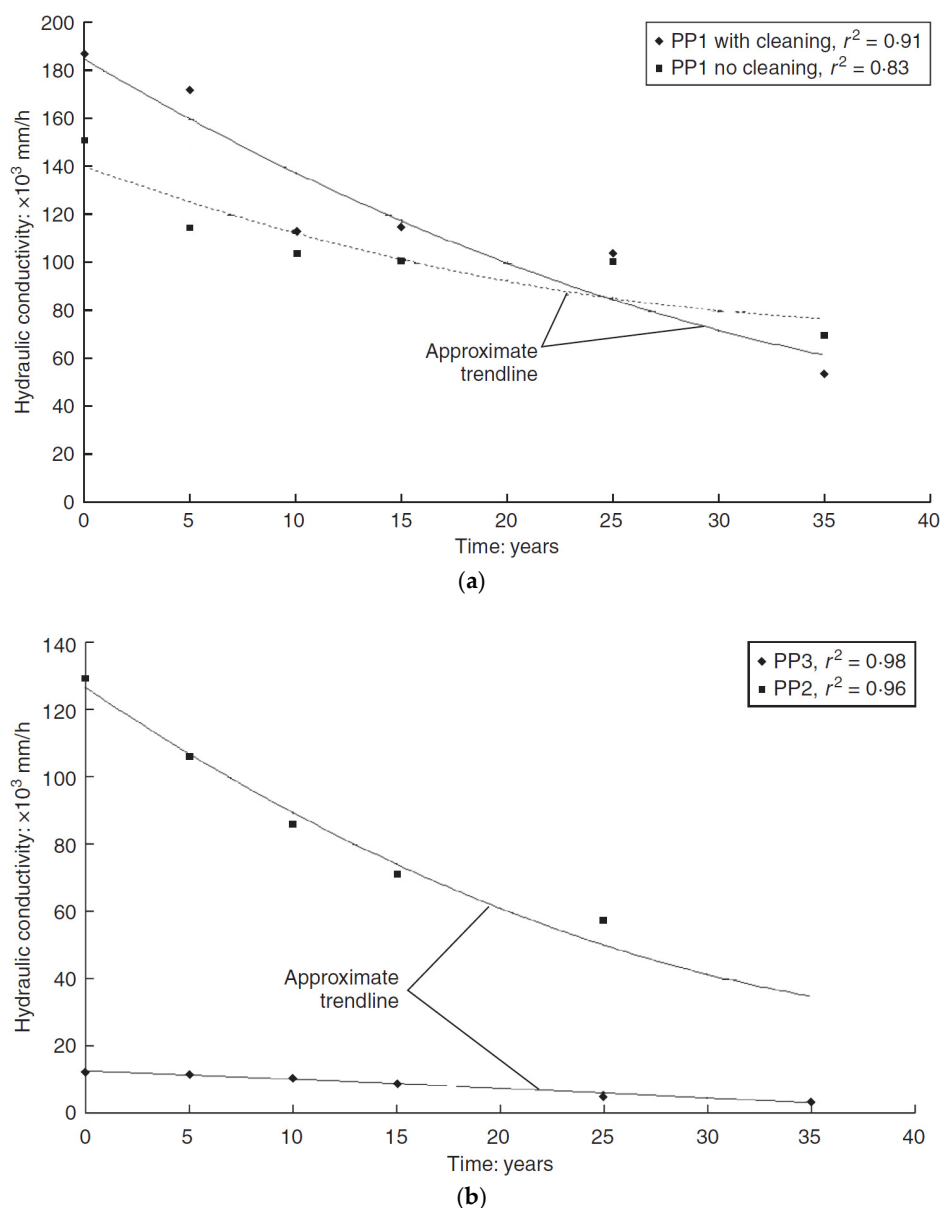


**Figure 2.** Changes in hydraulic conductivity over a simulated clogging period [6]: (a) The Boral Formpave bed (PP1); and (b) the Rocla Ecoloc (PP2) and Grasspave beds (PP3).

The authors [6] also conducted field infiltration tests on four sites using the “fitted tank”, depicted in Figure 1d. The test sites, Kirkcaldy Avenue and Victoria Park (PP1 installations), Fletcher Lane, Woodvile (PP2 installation), and St. Elizabeth Church, Warradale (PP3 installation), are located in the central business district of Adelaide. Field test results revealed a significant difference in the initial hydraulic conductivity values compared to those obtained from laboratory test results. This difference was attributed to the sediment that had accumulated between the time of installation and the period of testing.

Using the equipment shown in Figure 3, Fwa et al. [13,14] conducted laboratory tests to assess the drainage properties of different pavement materials including porous asphalt mixtures, following the principles of the falling head permeability test.

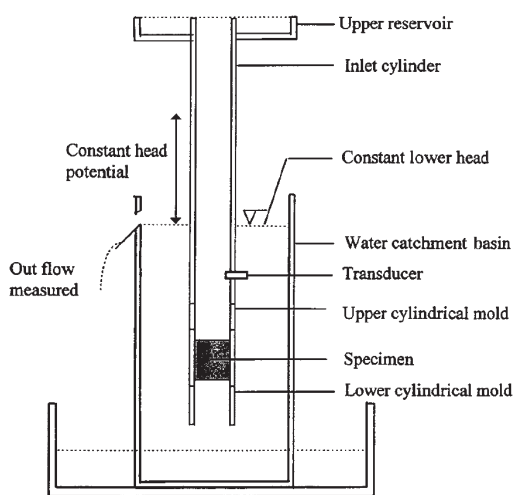


**Figure 3.** Falling head test apparatus setup [13].

For standard permeability tests on soils, the soil is normally assumed to exhibit laminar flow, and thus Darcy's law can be applied to evaluate the hydraulic conductivity. However, for pervious coarse-grained materials, the assumption of laminar flow is not valid. Several authors in the literature, including Fwa et al., have adopted the following relationship to describe the non-laminar flow conditions in pervious granular media, expressed as:

$$v = ki^n. \quad (1)$$

This equation is described as a modified Darcy's law, where  $k$  and  $n$  are the experimental coefficients. Typically,  $n$  varies from 1 to 0.5 for laminar to turbulent flows. For the permeability experiments conducted by Fwa et al.,  $k$  and  $n$  were obtained by plotting  $\log(v)$  against  $\log(i)$ , where the discharge velocity,  $v$ , and hydraulic gradient,  $i$ , were taken from the results of the falling head tests. After obtaining the experimental coefficients  $k$  and  $n$ , the authors found that the value of  $n$  could be taken as 0.7 for porous asphalt mixtures. Thus, the permeability coefficient,  $k$ , can be easily evaluated.

In 2017, Ahn et al. [15] developed a lab-scale apparatus for measuring the permeability of various pervious materials, which were not limited to pavement materials, but also to soils. Their apparatus (Figure 4) had more flexibility in terms of test methods, as it could perform both constant head and falling head permeability tests. Moreover, it could also evaluate the long-term hydraulic performance of pervious pavement materials by doing clogging simulations. The assessment of the permeability characteristics of polyurethane pavements was also described in their study. In addition, they performed falling head tests to evaluate the initial drainage properties of cylindrical samples, and the non-linear relationship between the discharge velocity,  $v$ , and the hydraulic gradient,  $i$ , was evident in their test results.

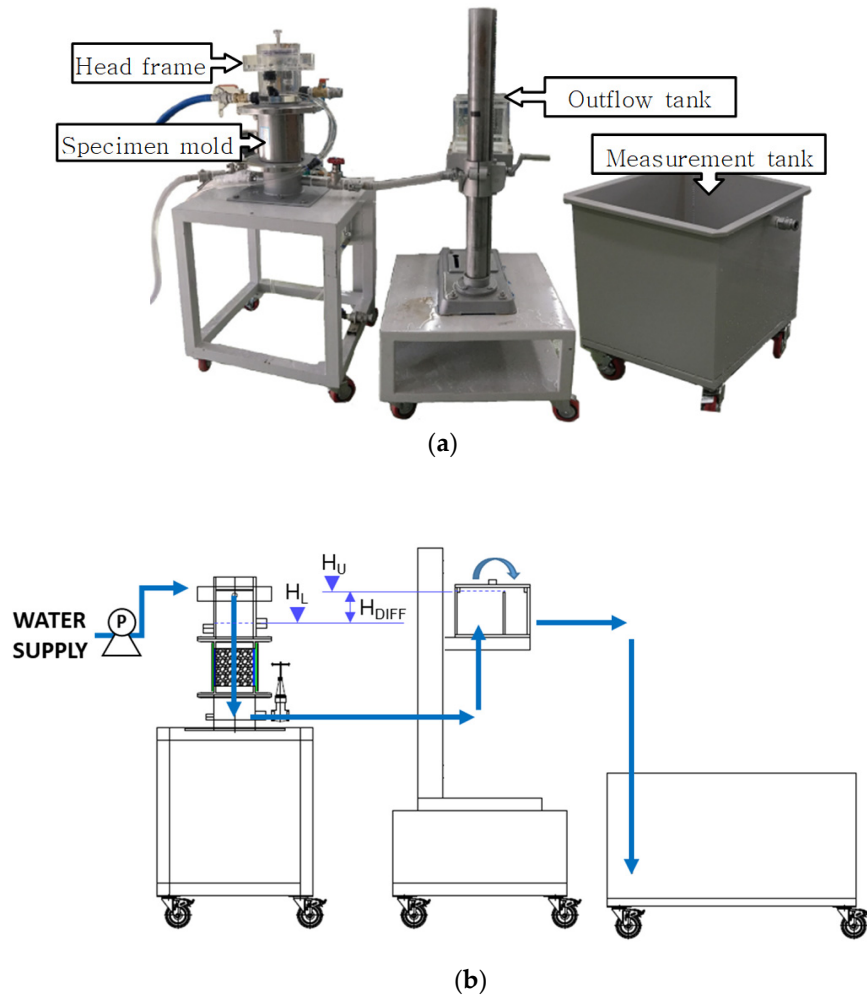


**Figure 4.** Permeability test apparatus [15]: (a) Parts and (b) schematic diagram.

Constant head permeability tests, coupled with clogging simulations, were also conducted to monitor the variations in the discharge velocity, in order to consider the effects of accumulated sand addition. Based on this experiment, it was discovered that the infiltration capacities of the specimens tested reduced by 50% after accumulating  $565 \text{ g/m}^2$  of clogging particles as shown in Figure 5. It was also observed that the degree of clogging was more gradual after accumulation of  $1700 \text{ g/m}^2$  of clogging particles.

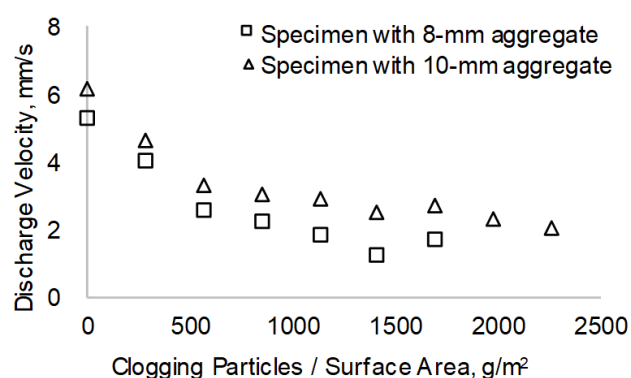


**Figure 5.** Clogging test results [15].

The studies reviewed above demonstrate the wide variety of findings that are possible from different investigations related to the hydraulic properties of permeable pavements. While studies have shown that the pavement performance—in terms of clogging—is dependent on a number of parameters [9,13,15–17,20,21], there are no established test procedures or standardized methods for evaluating the hydraulic capacity of a permeable pavement, especially in laboratory models [5,9]. This is particularly evident from the three pieces of literature widely reviewed here. The main objective of this study was to develop laboratory equipment which could investigate the changes in the hydraulic properties of permeable block pavements that result from simulated clogging processes. The changes in permeability were assessed to determine the quantity of fine sand that may contribute to hydraulic failure of the pavement system.

## 2. Materials and Methods

### 2.1. Equipment Development

A device was designed and developed for evaluation of the hydraulic properties of permeable pavement systems, as shown in Figure 6. The design employs the principles of the falling head method (FHM) and the constant head method (CHM) in measuring permeability characteristics. The permeability equipment was composed of a specimen mold, interchangeable head frames, an outflow tank, and a measuring tank. Usually, water was supplied into the head frame and was allowed to flow through the specimen. Pressure transducers were installed in the falling head frames and measuring tanks in order to detect changes in the water surface levels with time for the duration of the test. A data acquisition (DAQ) device was connected to the transducers to read signals and transmit data to a computer. Data obtained from pressure sensor readings provided the necessary information for computing the flow rates at any point in time during the test. For long-term performance evaluation, clogging particles were spread over the permeable pavement surface using an accessory called a particle distributor. The procedures used in operating the equipment are discussed in the following subsections.

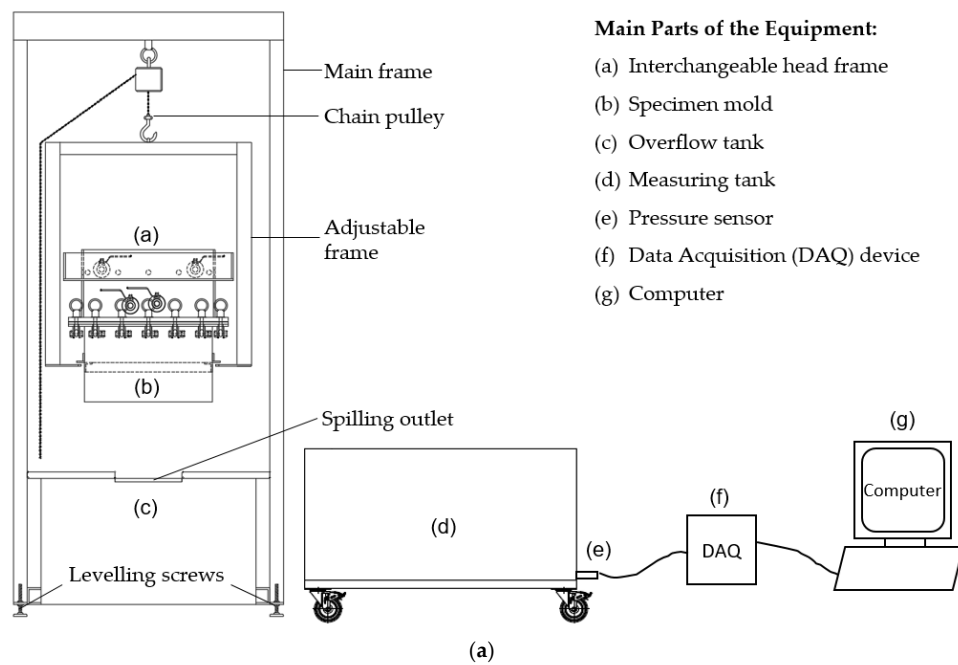
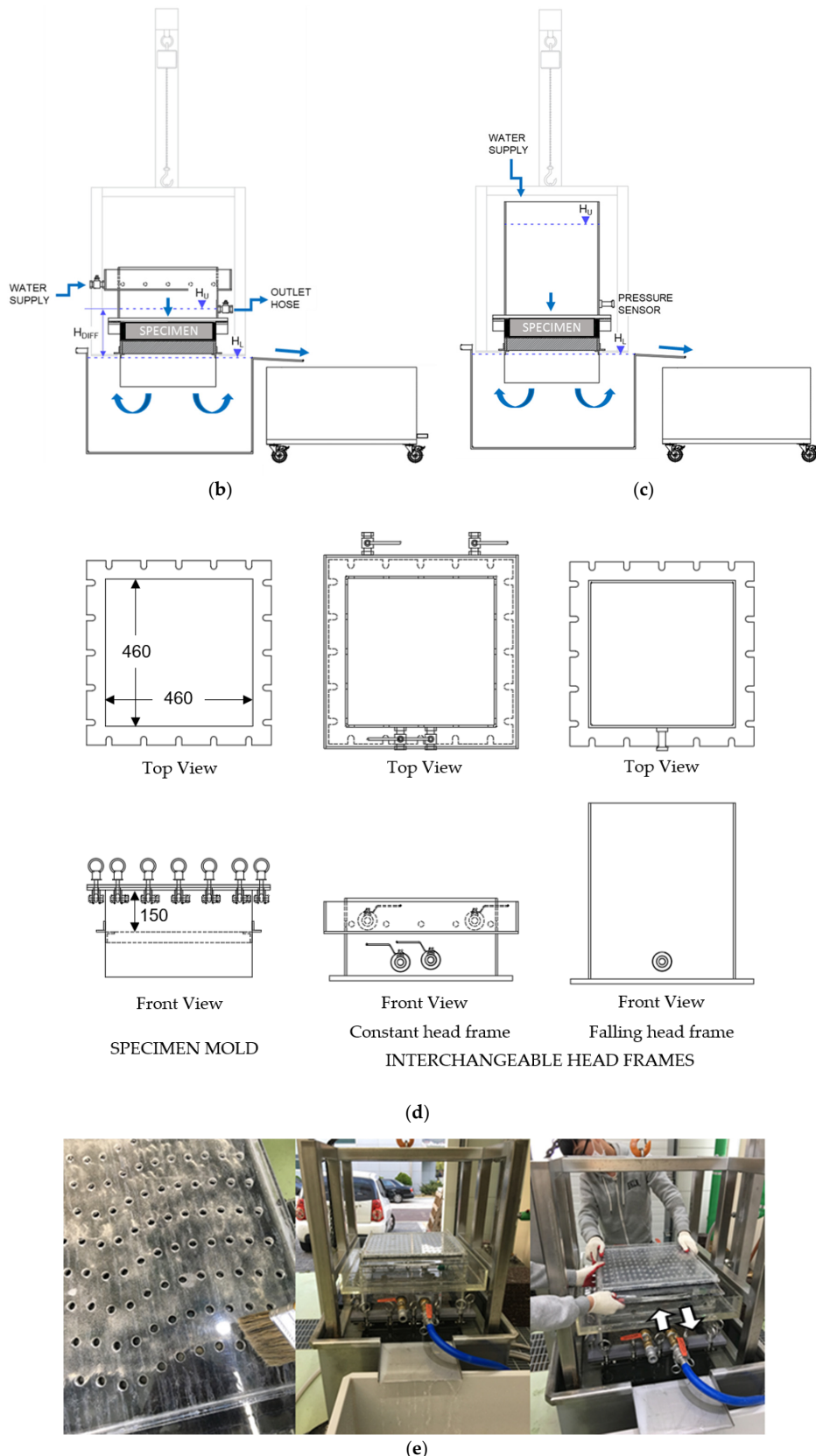


Figure 6. Cont.



**Figure 6.** Permeability test equipment for permeable block pavements: (a) Parts of the equipment; (b) schematic diagram of constant head permeability testing; (c) schematic diagram for falling head permeability testing; (d) details of equipment parts; and (e) clogging particle distributor.

## 2.2. General Procedures

### 2.2.1. Sample Preparation

Materials (Figure 7a):

- Specimen mold
- Permeable pavement sample with area =  $460 \times 460$  mm max. and thickness = 150 mm max.
- PVC frame with height = 150 mm (sample height)
- Perforated steel plate
- Rubber pieces with dimensions to suit sample dimensions
- Rubber gasket

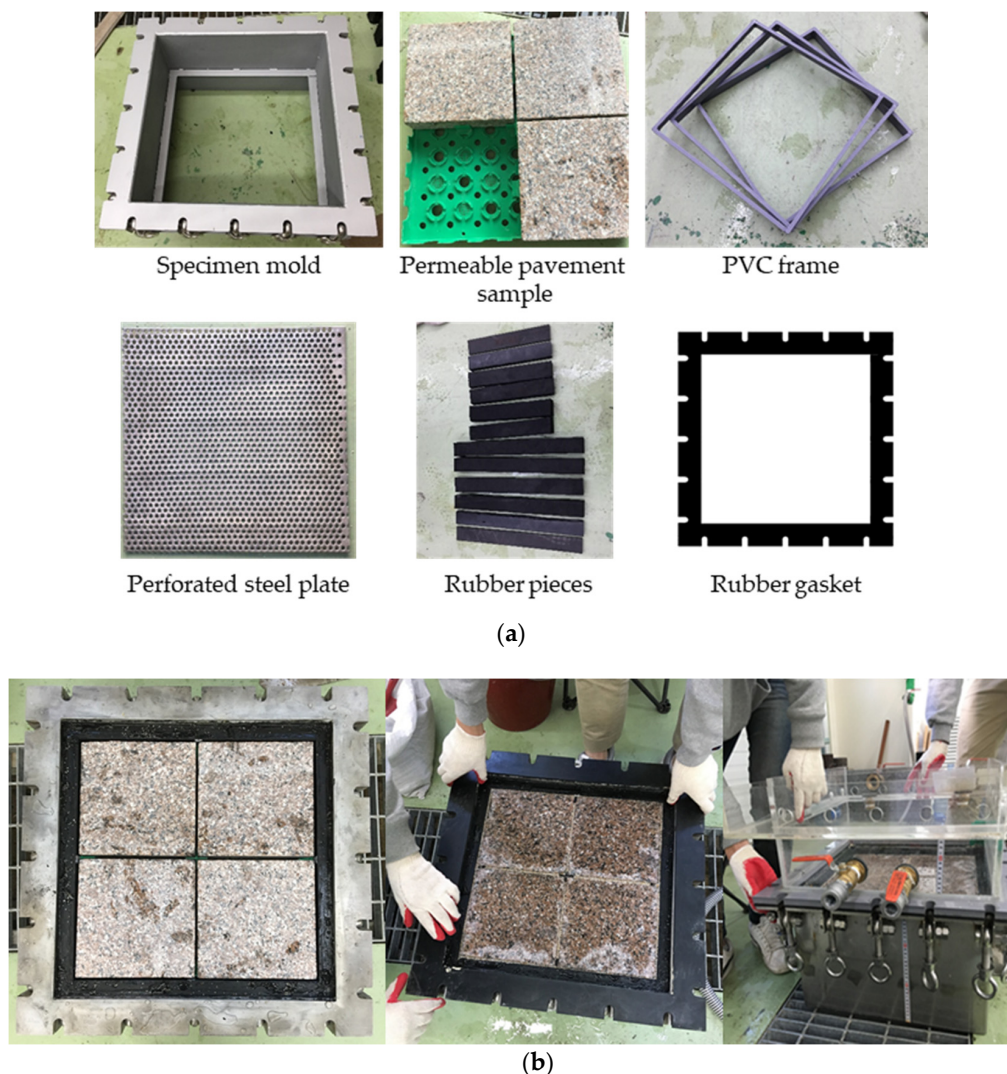


**Figure 7.** Specimen preparation: (a) Materials and (b) photos of study equipment.

Procedures (Figure 7b):

- (1) Place PVC frame inside the specimen mold.
- (2) Put the perforated plate on top of the PVC frame.

- (3) Arrange rubber pieces along the perimeter of the mold to secure the sample in the middle.
- (4) Secure the specimen in the space provided. Different types of pavement have different pavement layers. Assemble the pavement specimen based on its type (i.e., modular stone pavers used in this study have plastic base frame).
- (5) Seal the interface between the specimen mold and rubbers with silicone sealant to prevent leaks. Let this dry overnight.
- (6) Attach the rubber gasket to the top of the specimen mold.
- (7) Assemble the head frame of the desired permeability test above the gasket. Secure this in place by locking the bolts along the perimeter.

#### 2.2.2. Permeameter Assembly

- (1) Level the equipment by adjusting the levelling screws at the bottom of the overflow tank.
- (2) Place the specimen mold with the head frame onto the adjustable frame.
- (3) Place the measuring tank near the spilling outlet of the overflow tank.
- (4) Fill the overflow tank with water until the water reaches the spilling outlet.

#### 2.2.3. Constant Head Permeability Test

- (1) Connect a water supply to the inlet valve.
- (2) Connect a hose to the outlet valve.
- (3) Open the inlet and outlet valves.
- (4) Using the chain pulley, adjust the level of the specimen mold to a height that can achieve the desired hydraulic gradient (i.e., desired head difference).
- (5) Allow the water to flow through the sample until a stable head is established (i.e., there is no change in the higher and lower water levels).
- (6) With the aid of the DAQ device, record the volume of water collected in the measuring tank for a certain period of time.

#### 2.2.4. Falling Head Permeability Test

- (1) Using the chain pulley, adjust the level of the specimen mold at a height that can achieve the desired hydraulic gradient.
- (2) Fill the falling head frame with water at a desired upper water level.
- (3) Let the water drain through the sample.
- (4) With the aid of the DAQ device, attached to the falling head frame, record the time and height of water as the water level drops.

#### 2.2.5. Addition of Clogging Particles

- (1) Evenly spread a known amount of clogging particles onto the top layer of the particle distributor with the use of a brush.
- (2) Place the particle distributor onto the opening of the constant head frame.
- (3) Drop the clogging particles on to the specimen by dragging the second layer of the particle distributor in a push and pull manner.

#### 2.2.6. Permeability Test with Clogging Simulation

To monitor the changes in the hydraulic conductivity of the permeable pavement (due to clogging), a constant head permeability test was continuously conducted while the clogging process was simulated, as summarized in Figure 8.

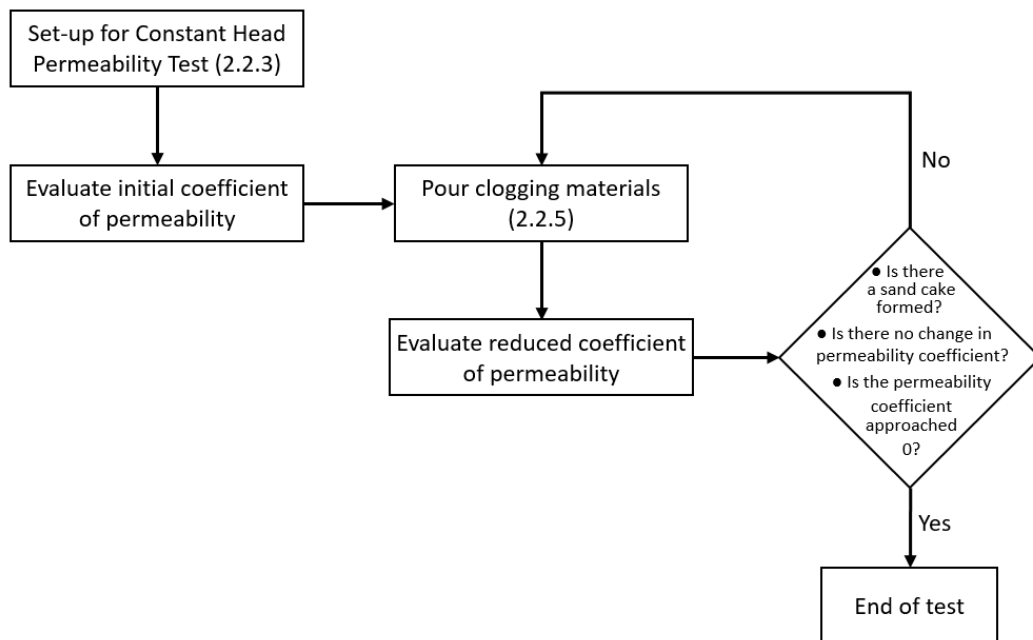


**Figure 8.** Flowchart for permeability test with clogging simulation.

### 2.3. Applications

This paper suggests a new piece of laboratory equipment and an associated procedure that can be used to characterize the flow properties and clogging potentials of permeable pavement materials. A project that was conducted to study the clogging behavior of a stone modular block pavement system—using the new equipment—is described in the next subsections. Permeability tests were conducted on three identical pavement block systems (PBS) to evaluate the drainage properties, including the discharge velocity and hydraulic conductivity, and to investigate the effects of particle deposition by adopting a clogging simulation procedure.

#### 2.3.1. Materials

A total of three permeable block systems (PBS) were used in this study, two of which were replicates. Each PBS consisted of four  $200 \times 200$  mm stone blocks assembled on a square high-density polyethylene (HDPE) base frame (Figure 7a). HDPE spacers kept the gaps between the blocks at a 5 mm width. Beneath the base frame, a 30 mm-thick layer of 0.85 to 2.0 mm diameter silica sand was laid as a bedding course. The bedding sand was held in place with a geotextile fabric laid on a perforated steel plate. The joints were then filled with the same material as the bedding sand.

Dry silica sand particles were used to simulate road dust particles. The amount of clogging sand used in the experiment was based on the quantity of fine particles collected from road dust sweepers in Seoul Metropolitan City, South Korea. Considering the distance travelled by the road sweeper vehicle and the lane width of the road, the concentration of particles amounts to  $0.06 \text{ g/cm}^2$  in five years. A mass of 20 g of silica sand was used to deliver the equivalent amount of clogging particles in one year to each specimen. Three different particle size distributions of silica sand were used to permeate the specimens. Their gradation curves are presented in Figure 9. The average sizes of the clogging particles (CP) for PBS 1, PBS 2, and PBS 3 were 0.14mm, 0.21mm, and 0.30mm, respectively. The CP sizes for PBS 1 and PBS 2 were chosen based on the size ratio of joint sand and clogging sand, and the CP size for PBS 3 was adopted from the gradation of the road dust particles collected from Seoul.

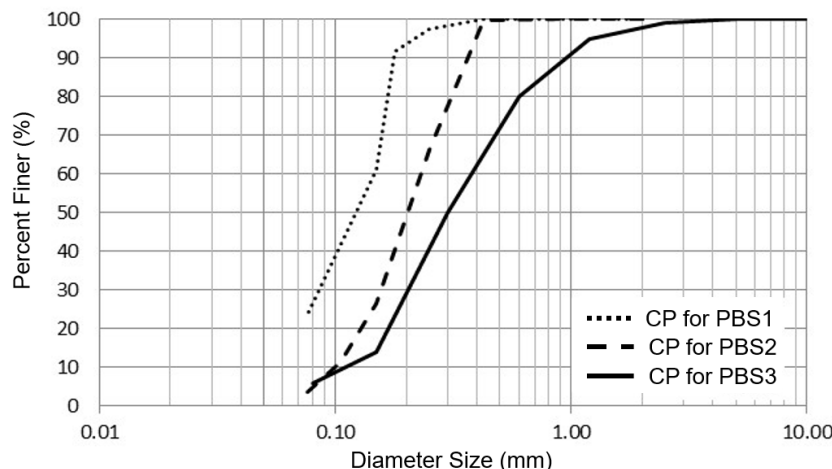


**Figure 9.** Particle size distribution of clogging particles (CP).

### 2.3.2. Test Details

Generally, in soil mechanics, the constant head test method is more suitable for porous materials, having high permeability, such as permeable pavement materials. In this study, the experiment was divided into two parts. The first part was the usual constant head permeability test, where the original permeability of the pavement system was evaluated. A minimum of five trials were conducted for each test specimen, with at least five minutes for each test duration.

The second part of the experiment consisted of a constant head permeability test with incremental addition of clogging particles, in order to evaluate the changes in the permeability characteristics of the test specimens due to particle deposition. Each model received the equivalent of eight years' worth of clogging particles during the entire experiment. The time interval before the next year's particles were applied was 10 min, to provide enough time for particle settling and brushing.

### 2.3.3. Computation of Permeability

Unlike other highly pervious materials, the hydraulic conductivity of the permeable pavement block system used in the experiment was governed by the joint and bedding sand. For permeability determination, Darcy's law was applied. According to Darcy, the rate of laminar fluid flow through a porous medium is proportional to the hydraulic gradient, resulting in the equation,

$$q = kiA, \quad (2)$$

where

$q$  = volumetric flow rate of water ( $\text{mm}^3/\text{s}$ );

$k$  = coefficient of permeability or hydraulic conductivity ( $\text{mm}/\text{s}$ );

$i$  = hydraulic gradient; and

$A$  = sample area ( $\text{mm}^2$ ).

The discharge velocity ( $\text{mm}/\text{s}$ ), defined as the quantity of fluid flow along the hydraulic gradient per unit cross sectional area, can be expressed as:

$$v = ki \quad (3)$$

In a constant head test, both time and water surface level are recorded at a maintained hydraulic gradient,  $i$ . Using simple linear regression, the discharge velocity,  $v$  can be determined from the slope. The coefficient of permeability,  $k$  can then be obtained by plotting values of  $i$  against  $v$ . The slope of the plot gives the value of  $k$ .

### 2.3.4. Computation of Reduced Permeability

The incremental addition of fine particles results in gradual reduction in permeability of the pavement block system. During the clogging test, the particles were added at an interval of 10 min. From the recorded data of time versus water surface level, the permeability could then be calculated at a desired time range. For this experiment, reduced  $k$  was computed within the last five minutes of the clogging time interval. The first five minutes were allotted for brushing and settling of particles.

## 3. Results

### 3.1. Coefficient of Permeability

Initial values of hydraulic conductivity ( $k$ ) of the bedding sand and three permeable pavement block systems (PBS) were evaluated. The bedding sand was tested first to verify the laminar condition of flow through the porous material using a smaller version of the equipment. The details of the small permeability equipment are discussed in the paper by Ahn et al. [15]. A total of eight constant head permeability tests were conducted at approximate hydraulic gradients of 0.5, 1.0, 1.5, and 2.0. The raw test data of the first trial for bedding sand is shown in Figure 10. The graph shows the change in the volume of water collected in the measuring tank with respect to time. A simple linear regression analysis was necessary to evaluate the permeability characteristics, specifically the discharge velocity,  $v$ , due to the noisy resolution of the raw data. In Figure 11, the discharge velocity data are plotted against the hydraulic gradient. Based on the regression line, it appears that the assumption of laminar flow did hold in the test, since the values reflect a linear relationship.

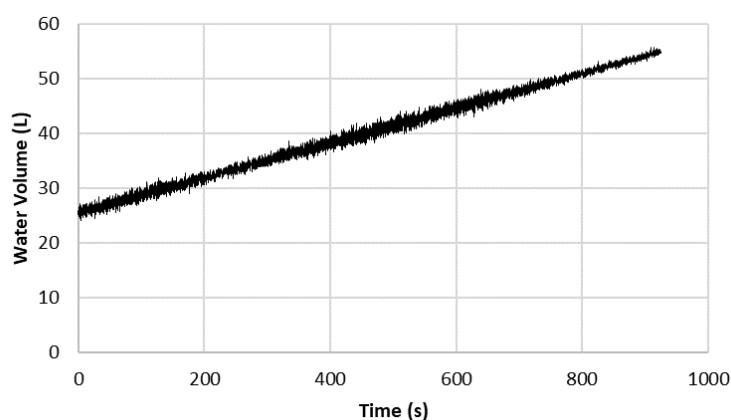


**Figure 10.** Raw test results for bedding sand ( $i \approx 0.5$ ).

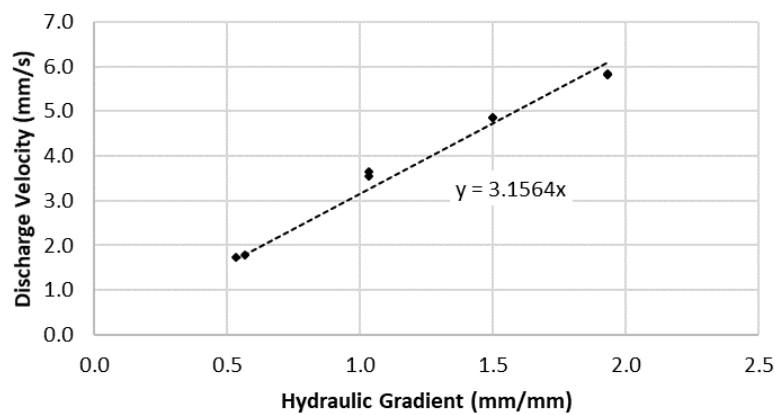


**Figure 11.** Constant head permeability test results for bedding sand.

For the evaluation of the permeability of PBS, only one hydraulic gradient was used for each specimen. The infiltration properties of PBS are mainly governed by bedding sand, and it was proven to behave as laminar. Thus, one hydraulic gradient was enough to evaluate the hydraulic conductivity of all the test specimens. The authors used a hydraulic gradient equal to 1.0 for all tests for PBS since  $k$  is equal to the value of  $v$  when  $i = 1.0$ . A minimum of five trials were conducted for each PBS. The raw test data of the first trial for PBS 1, PBS 2, and PBS 3 are presented in Figure 12. Based on the graph, the infiltration rate through the pavement block systems is slower compared to that of bedding sand. This may be attributed to the impermeable area covered by the stone pavers. The test results for the initial hydraulic conductivity evaluation are summarized in Table 2.

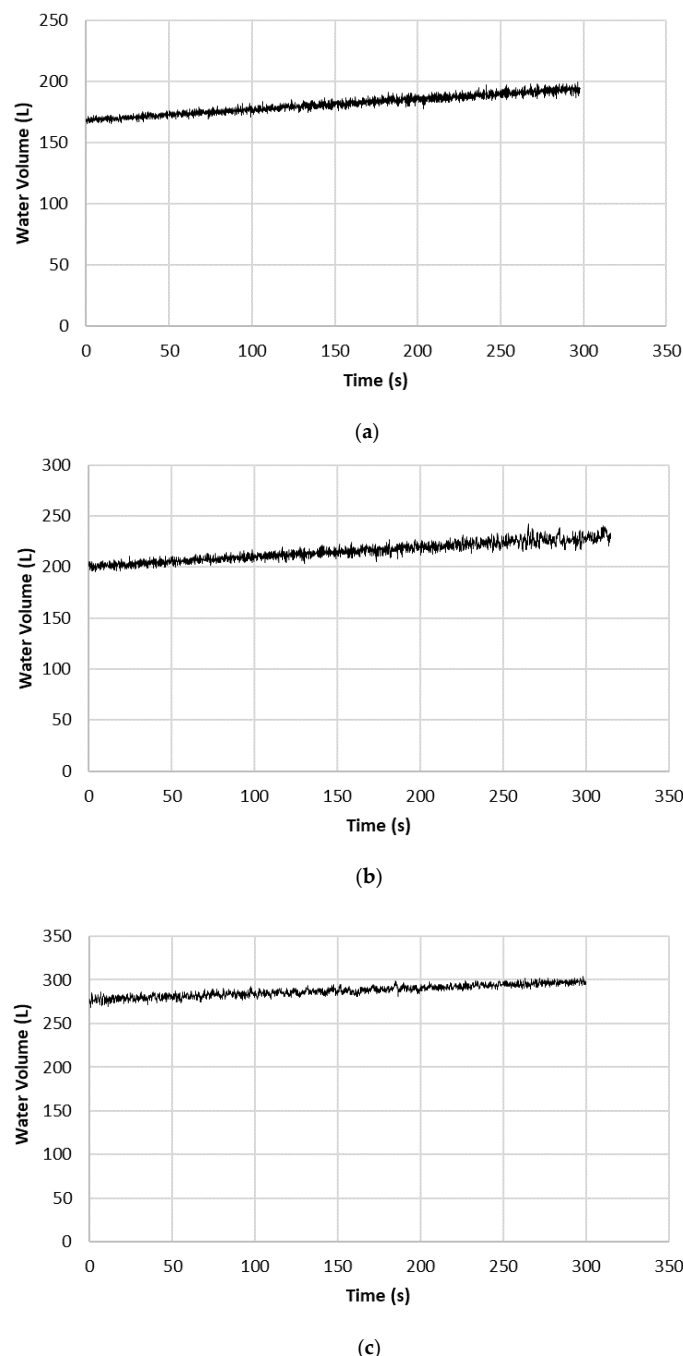


**Figure 12.** Raw test results from the first trial of each pavement block system (PBS): (a) PBS 1; (b) PBS 2; and (c) PBS 3.

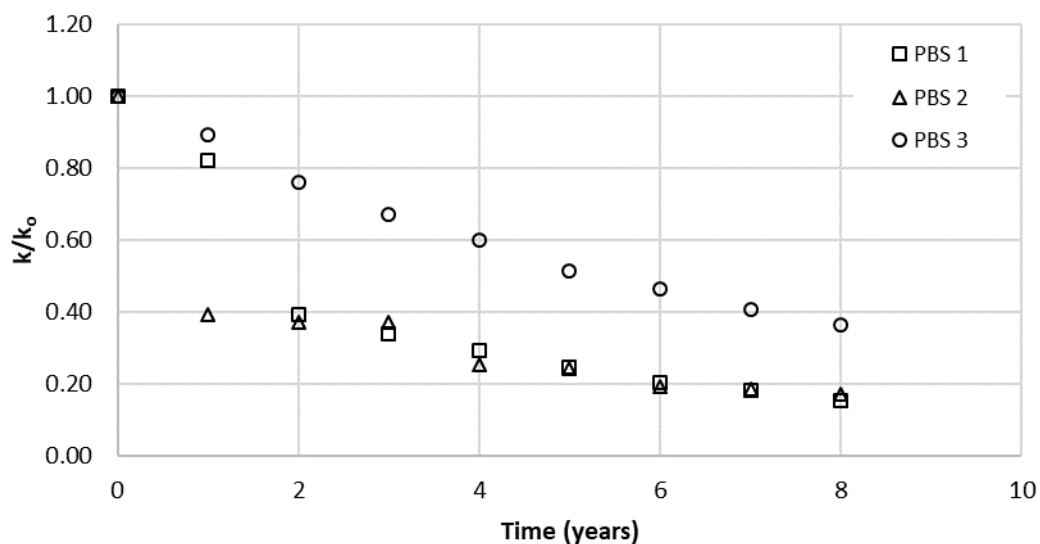
**Table 2.** Constant head test results for pavement block systems.

Trial	Initial Permeability Coefficient $k_o$ (mm/s)		
	PBS 1	PBS 2	PBS 3
1	0.58	0.475	0.406
2	0.488	0.498	0.443
3	0.537	0.546	0.409
4	0.442	0.496	0.408
5	0.508	0.548	0.408
6	0.549	0.555	0.418
7	0.453	0.52	-
8	0.517	-	-
Average	0.509	0.520	0.415
$^1 s$	0.044	0.029	0.013
$^2 s^2$	0.002	0.001	0.0002

$^1 s$  = standard deviation;  $^2 s^2$  = variance.

### 3.2. Reduced Permeability due to Clogging

The reduced permeability coefficients, normalized by the average initial permeability, were then plotted against the equivalent amount of clogging particles (in years), as shown in Figure 13. The graph shows the decline in hydraulic conductivity throughout the eight years of clogging without cleaning or maintenance. This represents an average reduction of 77%. The hydraulic conductivity of PBS 2 was similar to that of PBS 1, although the decline was more rapid. PBS 3 exhibited an order of magnitude higher than the other two pavements under test. The hydraulic conductivity of PBS 3 declined by 64%, whereas PBS 1 and PBS 2 reached more than 80%. Compared to PBS 1 and PBS 2, the clogging particles used to permeate PBS 3 contained more larger-sized particles. Due to the presence of these larger-size particles, a significant amount of the clogging sand was prevented from entering through the pores on the surface. For PBS 1 and PBS 2, the clogging particles used were finer, which made them more likely to infiltrate through the voids on the surface. PBS 1 had the smallest clogging particle size, and thus PBS 1 took more time to eventually clog compared with PBS 2. From this, it may be deduced that the amount of particles susceptible to pore infiltration affects the degree of pavement clogging.

**Figure 13.** Permeability reduction due to clogging.

#### 4. Conclusions

Due to the limited methods and equipment available for evaluation of hydraulic performance of permeable pavement materials, this paper proposes a newly designed and developed piece of laboratory equipment that is capable of measuring the hydraulic properties of permeable pavement materials, such as discharge velocity and the coefficient of permeability. The details of this device and the operational procedures have been outlined in the early sections of this paper. The authors have also suggested a method for evaluating the long-term performance of permeable pavement, by simulating a surface clogging process.

As described in this paper, an investigation into the effects of particle clogging on the long-term performance of a modular permeable block system—using the proposed laboratory equipment and clogging method—was carried out. The main outcome of the experiment reflected the decline of the system's drainage capacity relative to its original hydraulic properties. It was found that the initial values of hydraulic conductivity measured using the equipment are fairly consistent for all the test specimens. In addition, the results from the permeability test in conjunction with the clogging simulation revealed a good agreement with the infiltration rate trends that are demonstrated in the existing literature. Based on this, the proposed laboratory apparatus and its associated long-term permeability assessment method may be considered as a reliable tool for evaluating the hydraulic performance of pervious materials.

**Author Contributions:** J.A. designed and developed the test equipment. J.A., A.K.M., Y.L. and J.J. conceived the experimental program, performed the experiments, analysed the data, and wrote the paper. All authors read and approved the final manuscript.

**Funding:** This research was supported by a grant from Technology Advancement Research Program (grant No. 18CTAP-C132363-02) funded by the Ministry of Land, Infrastructure, and Transport of Korean government.

**Acknowledgments:** The authors would like to thank the Ministry of Land, Infrastructure, and Transport of Korean government for the grant from Technology Advancement Research Program (grant No. 18CTAP-C132363-02).

**Conflicts of Interest:** The authors declare no conflicts of interest.

#### References

1. Lucke, T.; Beecham, S. Field investigation of clogging in a permeable pavement system. *Build. Res. Inf.* **2011**, *39*, 603–615. [[CrossRef](#)]
2. Lucke, T. Using drainage slots in permeable paving blocks to delay the effects of clogging: Proof of concept study. *Water* **2014**, *6*, 2660–2670. [[CrossRef](#)]
3. Sañudo-Fontaneda, L.A.; Rodriguez-Hernandez, J.; Vega-Zamanillo, A.; Castro-Fresno, D. Laboratory analysis of the infiltration capacity of interlocking concrete block pavements in car parks. *Water Sci. Technol.* **2012**, *67*, 675–681. [[CrossRef](#)] [[PubMed](#)]
4. Booth, D.; Leavitt, J. Field evaluation of permeable pavement systems for improved stormwater management. *J. Am. Plan. Assoc.* **2007**, *65*, 314–325. [[CrossRef](#)]
5. Lucke, T.; Boogaard, F.; van de Ven, F. Evaluation of a new experimental test procedure to more accurately determine the surface infiltration rate of permeable pavement systems. *Urban Plan. Transp. Res.* **2014**, *2*, 22–35. [[CrossRef](#)]
6. Pezzaniti, D.; Beecham, S.; Kandasamy, J. Influence of clogging on the effective life of permeable pavements. *Proc. Inst. Civ. Eng. Water Manag.* **2009**, *162*, 211–220. [[CrossRef](#)]
7. Aryal, R.; Beecham, S.; Lee, B. Evaluation of particle transport in permeable pavements under oil loadings. *KSCE J. Civ. Eng.* **2015**, *19*, 2000–2004. [[CrossRef](#)]
8. Van Duin, B.; Brown, C.; Chu, A.; Marsalek, J.; Valeo, C. Characterization of long-term solids removal and clogging processes in two types of permeable pavement under cold climate conditions. In Proceedings of the 11th International Conference on Urban Drainage, Edinburgh, UK, 31 August–5 September 2008.
9. James, W. Clogging of permeable concrete block pavement by street particulates and rain. *J. Water Manag. Model.* **2004**, *12*. [[CrossRef](#)]

10. Abdollahian, S.; Kazemi, H.; Rockaway, T.; Gullapalli, V. Stormwater quality benefits of permeable pavement systems with deep aggregate layers. *Environments* **2018**, *5*, 68. [[CrossRef](#)]
11. Braswell, A.; Anderson, A.; Hunt, W. Hydrologic and water quality evaluation of a permeable pavement and biofiltration device in series. *Water* **2018**, *10*, 33. [[CrossRef](#)]
12. Sañudo-Fontaneda, L.; Andres-Valeri, V.; Costales-Campa, C.; Cabezon-Jimenez, I.; Cadenas-Fernandez, F. The long-term hydrological performance of permeable pavement systems in northern Spain: An approach to the “end-of-life” concept. *Water* **2018**, *10*, 497. [[CrossRef](#)]
13. Fwa, T.; Tan, S.; Chuai, C. Permeability measurement of base materials using falling-head test apparatus. *Transp. News Rec.* **1998**, *1615*, 94–99. [[CrossRef](#)]
14. Fwa, T.; Tan, S.; Guwe, Y. Laboratory evaluation of clogging potential of porous asphalt mixtures. *Transp. Res. Board* **1999**, *1681*, 43–49. [[CrossRef](#)]
15. Ahn, J.; Jalmasco, M.; Shin, H.; Jung, J. Test equipment and procedure to evaluate permeability characteristics of permeable pavements. *J. Korean Soc. Hazard. Mitig.* **2017**, *17*, 359–365. [[CrossRef](#)]
16. Yong, C.F.; McCarthy, D.T.; Deletic, A. Predicting physical clogging of porous and permeable pavements. *J. Hydrol.* **2013**, *481*, 48–55. [[CrossRef](#)]
17. Brown, R.; Borst, M. Assessment of clogging dynamics in permeable pavement systems with time domain reflectometers. *J. Environ. Eng.* **2013**, *139*, 1255–1265. [[CrossRef](#)]
18. Støvring, J.; Dam, T.; Bergen Jensen, M. Surface sedimentation at permeable pavement systems: Implications for planning and design. *Urban Water J.* **2018**, *15*, 124–131. [[CrossRef](#)]
19. Boogard, F.; Lucke, T.; van de Giesen, N.; van de Ven, F. Evaluating the infiltration performance of eight dutch permeable pavements using a new full-scale infiltration testing method. *Water* **2014**, *6*, 2070–2083. [[CrossRef](#)]
20. Hill, K.D.; Beecham, S. The effect of particle size on sediment accumulation in permeable pavements. *Water* **2018**, *10*, 403. [[CrossRef](#)]
21. Andres-Valeri, V.; Marchioni, M.; Sañudo-Fontaneda, L.; Giustozzi, F.; Becciu, G. Laboratory assessment of the infiltration capacity reduction in clogged porous mixture surfaces. *Sustainability* **2016**, *8*, 751. [[CrossRef](#)]



© 2018 by the authors. Licensee MDPI, Basel, Switzerland. This article is an open access article distributed under the terms and conditions of the Creative Commons Attribution (CC BY) license (<http://creativecommons.org/licenses/by/4.0/>).